Modeling RF Propagation in Tunnels

Chenming Zhou, Joseph Waynert,Timothy Plass, and Ronald Jacksha
Office of Mine Safety and Health Research
National Institute for Occupational Safety and Health
Pittsburgh, PA 15236, USA
czhou@cdc.gov, jwaynert@cdc.gov, tplass@cdc.gov, rjacksha@cdc.gov

***Abstract*— As mandated by the 2006 Mine Improvement and New Emergency Response (MINER) Act, many underground coal mines have installed UHF radio systems to provide communications between personnel on the surface and underground. In an effort to better understand UHF signal propagation in tunnel environments, we made radio signal attenuation measurements in concrete tunnels at frequencies of 455 MHz, 915 MHz, 2.45 GHz, and 5.8 GHz. In this paper, a ray tracing method is used to model the channel. Although the tunnel has an arched roof, the model describes the propagation behavior very well using a rectangular tunnel with the same width. The measured data verify the ability of the ray tracing model to predict radio frequency propagation at all the four frequencies. In addition, the propagation constants for the different frequencies are investigated and shown to be consistent with the measured values.**

Keywords—Waveguide, tunnel propagation, ray tracing, attenuation constant.

I. INTRODUCTION

RF propagation in tunnel environments has been an active research topic for decades [1-5]. A renewed interest was recently spurred by the MINER Act which requires wireless communication systems be installed in all U.S. underground coal mines [4]. The performance of these wireless systems is highly dependent on the radio propagation behavior in the confined environment of tunnels typical of a coal mine. Therefore, effective prediction tools and models are critical in the design phase of the system.

In an effort to better understand the parameters that control RF propagation, we made radio signal attenuation measurements in tunnels at frequencies of 455, 915, 2450, and 5800 MHz, which are common frequencies for commercially available systems. In this paper, we will first briefly describe our measurements and then use a ray approach to model the channel.

II. MEASUREMENT

RF power measurements were made along a straight concrete tunnel. The tunnel is rectangular with an arched ceiling as shown in Fig. 1 (a). The length of tunnel is about 610 m. Two identical linear polarized antennas were used at the transmitter and receiver, and were set to the same height of 1.22 m. The antennas were located in the center between the two side walls during measurements. More details about our measurements can be found in [5].

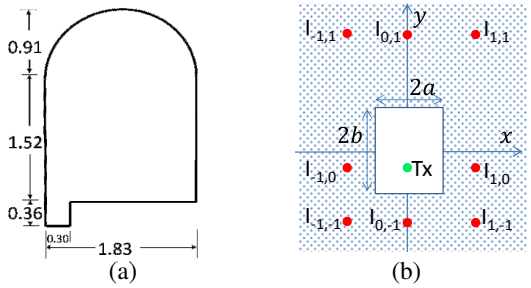

Figure 1. Geometry of the tunnel. (a) shows the dimensions of the tunnel cross section in meters and (b) illustrates the images of the source within the tunnel.

III. RAY TRACING BASED CHANNEL MODEL

A. Image theory

We approximate the cross section of the tunnel in Fig. 1(a) with a rectangle of the same width and a height of 2.35 m. The coordinate system is assumed to be centered in the tunnel, with x horizontal, y vertical, and z down the tunnel, as illustrated in Fig. 1 (b). An arbitrary point source is located in $Tx\ (x_0, y_0, z_0)$, and the location of an image $I_{m,n}$ can be obtained as:

$$\begin{aligned} x_m &= 2ma + (-1)^m x_0 \\ y_n &= 2nb + (-1)^n y_0 \end{aligned} \tag{1}$$

where $2a$ and $2b$ are the width and height of the rectangle, respectively. The integers m and n correspond to the number of reflections that the ray undergoes relative to the horizontal and vertical walls, respectively. The sign of m and n indicate whether the image is located at the positive or negative x and y axis, respectively.

B. Electric field in a rectangular waveguide

For a vertical polarized source, the electric field at the point $R(x, y, z)$ in the far field ($z \gg \max(2a, 2b)$) can be obtained by summing the scalar electric fields of the rays from all the images of the point source as [3]:

$$E_r(x, y, z) = E_t \sum_{m=-\infty}^{+\infty} \sum_{n=-\infty}^{+\infty} \frac{e^{-jkr_{m,n}}}{r_{m,n}} \rho_{\perp}^{|m|} \rho_{//}^{|n|} \tag{2}$$

where E_t is the transmitted electric field, k is the wave number in the waveguide, and $r_{m,n}$ is the distance between the receiver and the image $I_{m,n}$, and is given by :

$$r_{m,n} = \sqrt{(x_m - x)^2 + (y_n - y)^2 + z^2} \tag{3}$$

$\rho_{\perp,//}$ represent the perpendicular and parallel reflection coefficients respectively, and are given by:

$$\rho_{\perp} = \frac{\cos\theta_i - \sqrt{\bar{\varepsilon} - \sin^2\theta_i}}{\cos\theta_i + \sqrt{\bar{\varepsilon} - \sin^2\theta_i}} \qquad \rho_{//} = \frac{\bar{\varepsilon}\cos\theta_i - \sqrt{\bar{\varepsilon} - \sin^2\theta_i}}{\bar{\varepsilon}\cos\theta_i + \sqrt{\bar{\varepsilon} - \sin^2\theta_i}} \qquad (4)$$

where θ_i is the incidence angle relative to a normal to the reflecting surface. The value of θ_i can be readily obtained by $\theta_i = \text{acos}\left(|y_n - y|/r_{m,n}\right)$ and $\theta_i = \text{acos}\left(|x_m - x|/r_{m,n}\right)$ for the parallel and perpendicular polarization, respectively. $\bar{\varepsilon}$ is the ratio of the complex dielectric constant of the two media separated by the reflection interface. For a hollow rectangular tunnel, we have $\bar{\varepsilon} = \varepsilon_r - j\sigma/(2\pi f \varepsilon_0)$, where f is the frequency and ε_0 is the dielectric constant of air. Here ε_r and σ are the relative dielectric constant and conductivity of the tunnel walls, respectively. It should be noted that in a practical environment the value of ε_r and σ could be different for walls as compared to the roof and floor of the tunnel. Omni-directional antennas are assumed in (2).

IV. Results

Simulation and measurement comparison: Fig. 2 shows a comparison between the measured results and the simulated results at different frequencies for the vertically polarized transmitter and receiver. The blue solid line represents the measured results and the red dotted line the simulated results based on the ray tracing model described in Section III. The same electrical constitutive parameters ($\varepsilon_r = 8.9$ and $\sigma = 0.15$ S/m) are used for both the vertical and horizontal walls of the tunnel. It was found that contributions from the rays that undergo more than 40 reflections are negligible. Therefore, the absolute values of both *m* and *n* in (2) have been limited to 40.

Attenuation constant: In Figs 2 (a), (b), and (c), it is observed that the signal (when plotted in a dB scale) attenuates linearly with the distance in the far field. At each frequency, the attenuation slope can be calculated based on the linear least squares fitting, for both the simulated and measured results. A comparison of the attenuation constant (slope) at different frequencies is shown in Fig. 3. An analytical result calculated based on the attenuation constant of the dominant EH_{11} mode in [2] is also plotted for reference. The same electrical parameters are used for the simulated (ray tracing based) and analytical results. It is shown that the simulated, measured, and analytical results agree well with each other. Note that fluctuations are observed in the simulated attenuation constant at the high frequency region. This is due to the fact that significant nulls exist along the tunnel (e.g, see Fig. 2 (d)) when the frequency of the signal is high. The presence of the nulls increases the uncertainty in the determination of the best linear fitting to the data.

V. Conclusion

A ray tracing model is developed to predict radio propagation in tunnels. The model predictions are validated by measurements at the four frequencies that are commonly used in commercially available communication systems. The model developed is useful for designing better communication and tracking systems in tunnel-like environments such as an underground coal mine.

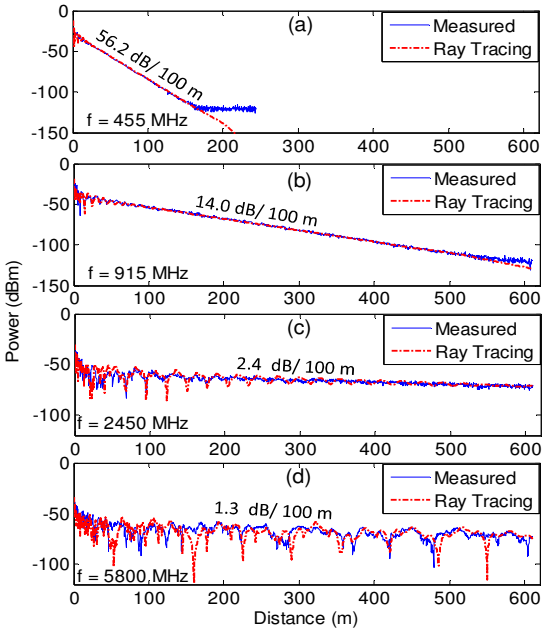

Figure 2. Comparison between the measured and the simulated power within a rectangular tunnel at different frequencies.

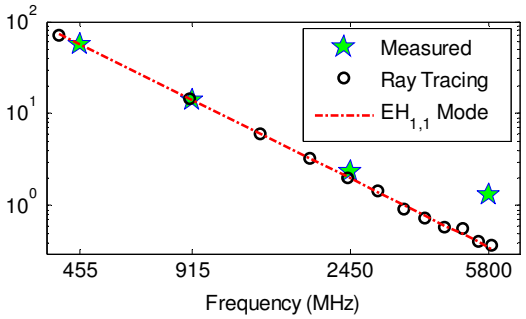

Figure 3. Comparsion between the measured and simuated attenuation slope at different frequncies. An analytical result calculated based on the attenuation constant of the dominant EH_{11} mode in [2] is also plotted for reference. Note that both of the axises are shown in a logarithmic scale.

Disclaimer: The findings and conclusions in this paper are those of the authors and do not necessarily represent the views of the National Institute for Occupational Safety and Health (NIOSH).

References

[1] R. A. Farmer, and N. H. Shepherd, "Guided radiation…the key to tunnel talking," IEEE Transactions on Vehicular Communications, vol. 14, No. 1, pp. 93–102, March, 1965.

[2] A. G. Emslie, R. L. Lagace and P. F. Strong, " Theory of the propagation of UHF radio waves in coal ine tunnels," IEEE Transactions on Antenna and Propagation," Vol 23., No. 2, pp. 192–205, March, 1975.

[3] Z. Sun and I. F. Akyildiz, "Channel modeling and analysis for wireless networks in underground mines and road tunnels," IEEE Transactions on Communications, vol. 58, No. 6, pp.1758–1768, June, 2010.

[4] United States Public Laws, PL 109-236, *Mine Improvement and New Emergency Response Act of 2006 (MINER Act)*, Jun. 15, 2006.

[5] T. Plass, R. Jacksha, J. Waynert, and C. Zhou, "Measurement of RF Propagation in Tunnels,' Submitted to IEEE Symposium on Antenna and Propagation (APS2013).